Determination of tensile strength of electrospun single nanofibers through modeling
tensile behavior of the nanofibrous mat

Molnár K., Vas L. M., Czigány T.

# TESTING AND MODELING THE TENSILE PROCESS OF ELECTROSPUN NANOFIBROUS MATS

Kolos MOLNAR[1a], László Mihály VAS[1] and Tibor CZIGANY[1]
[1]Department of Polymer Engineering, Faculty of Mechanical Engineering,
Budapest University of Technology and Economics. Műegyetem rkp 3., H-1111
Budapest, Hungary
[a] e-mail: molnar@pt.bme.hu, tel: 0036/1-463-1487, fax: 0036/1-463-1527

**Abstract**

The mechanical properties of poliamide-6 (PA-6) electrospun nanofibrous mat samples were tested. With the aid of the previously developed modeling software the whole tensile process was analyzed. The structural changes under the tensile process were evaluated from the modeling results and also compared to scanning electron micrographs. It was found that above a critical stress value nanofibers are slipping on one another which play an important role as well as the changes in the fiber orientation during the process. With the aid of the modeling software the tensile strength of single nanofibers under ideal in-axis stress and ideal gripping circumstances were estimated. It was found that single nanofibers have 48 percent higher tensile strength than the bulk PA-6 material has.

## 1. Introduction

### 1.1. Electrospinning

Investigation of the mechanical properties of nanomaterials is a very wide and popular research area nowadays [1-3] because of their unique properties. This statement is also valid for electrospun nanofibers. Electrospinning has gained high interest in the last two decades because it provides a cost-effective and versatile single-step method to produce nanofibrous structures. The fiber diameters can easily be varied by the process

parameters usually from 50 nm up to a few hundred nanometers. The product is more often a fiber mat, but with special electrode set-ups other structures can be obtained, as well as mats with oriented fibers [4], yarns [5-7] etc. [8]. Electrospun nanofibers can also be combined with carbon nanotubes [9] and/or different types of fillers [10] as well as drugs [11-12] and moreover the surface of the fibers can also be modified for further functionalization with the aid of for example plasma treatment and surface grafting [13]. Composite nanofibers can also be produced which can also be functionalized [14].

In the basic electrospinning set-up a high voltage power supply is connected to two electrodes: the spinneret and the collector, where more often the former one is under high voltage, the latter one is grounded. Electrospinning uses electrostatic forces to draw the fibers. A polymer solution or droplet is formed on the spinneret electrode, which can be supplied by glass pipette or syringe pump [8], etc.

Nanofibrous mat structures are consist of fibers, which can be considered as endless, because their length is orders of magnitude higher than their diameter. It is because of the fibers formation during the electrospinning process (thin jet which emerges from the tip of the Taylor-cone, then travels and elongates to the collector and bears different instabilities). This statement can be easily confirmed for example by SEM, because no fiber endings can be seen in the micrographs.

The whipping and bending instabilities of the just-forming fibers is pointed out by Reneker and Yarin [15] in detail. During fiber formation fibers twist and swirl each other as they travel to the collector electrode. They can also stick together if they contact in liquid phase which is usual because of the bending and whipping instabilities. Therefore the structure which is formed on the surface of the metal plate collector is a nonwoven mat: potentially endless fibers with bondings between them. The structure

can be expressed with the fiber orientation, fibers average diameter, the deviation of fiber diameters, the density and quality of bonding between the fibers, etc. as structural parameters.

There are several ways to measure the mechanical properties of single nanofibers [16-18], but these methods require special and also expensive apparatus, for example atomic force microscopy, micromanipulators, etc. That is the reason why testing of nanofibers is usually limited to the determination of geometrical or drug release properties. The tensile stress of single fibers is a key parameter for designing and sizing nanofibrous structures, such as composites or even filtration media.

In our research, the aim was to find a method which can approximate the mechanical properties of single nanofibers without using any special test device or special sample preparation method and to reveal the structural changes of nanofibrous mats along the whole tensile process.

### 1.2. Modeling Background

The fibers within oriented structures, such as yarns or rovings can be different from the straight, well-gripped, ideal fiber as for example oblique, crimped, etc. fibers can take part in real structures. The fibers can be classified according to their geometrical properties. These fiber classes are called fiber-bundle-cells (FBCs) [19]. Each FBC represent a set of fibers with mechanical, geometrical, etc. parameters as statistical and random variables. It is assumed that fibers are ideally elastic.

The *E-bundle* consists of straight fibers located parallel with the axis of pulling. These fibers are modeled as ideal springs, so the strain is directly proportional with the stress. The *EH-bundle* consists of positive or negative pre-stressed (crimped, wavy) fibers. The chord of bundle determined by the two ends is parallel with the axis of pulling. The *ET-*

*bundle* consists of straight, but oblique fibers. In case of E, EH, ET cells all fibers are ideally-gripped at both ends, what mean they can not slip out of the grips.

The *ES-bundle* can be defined as straight elastic fibers parallel with the axis of pulling, but can create fiber-chains with slipping connections, which also presents itself in the pulling force because of the friction between the fibers. The schemes of these FBCs are shown in Fig.1. [20].

With the aid of FBCs, nonwoven mat structures can also be expressed, in this case ET (oblique) FBCs with appropriate orientation angles should be used, and although in these structures other FBCs can also be imagined parallel to the ET type.

Modeling software (FiberSpace) which is based on idealized FBCs was developed by Vas et al. [21-23]. It works with statistical parameters of the FBCs, such as: the relative fracture of fiber cells within the specimen, the deviation of the fibers strain at break, the average fiber obliquity and its deviation, the average pre-stress of fibers and its deviation, etc. as modeling parameters. The software automatically tries to minimize the difference between the tensile curve destined for modeling and the resulting curve by iteration of more than 15 statistical parameters. As the best-fitting curve is found the parameters can be saved and with their air the structural and mechanical properties can be concluded.

For the modeling usually the average tensile curve is used. It means that the stress values of many measurements are added together as a function of strain and then the values are divided by the number of total measurements. This method is applied because the average of the high number of measurements usually gives more information about the structure than a result of only one measurement.

## 2. Materials and Methods

PA-6 (Schulamid 6MV13F) granulate was dissolved in 85 w% formic acid (REANAL ZRt, Hungary) and had a concentration of 16 w% which was selected on the basis of former results [24]. A magnetic mixer was used for stirring at a temperature of 60 °C, approximately for 3 hours.

Nanofibers were prepared by almost a classical electrospinning set up, but the collector was a rotating drum. It is applied because in case of a plate collector a patch of nanofibers can be created, but the surface density within the sample is not homogeneous, the cross-section has a high deviation [24]. With a rotating drum this problem can be avoided, because in that case the linear density of the sample is constant in the direction of rotation. The samples were produced for 2 hours and at low rotation speeds, therefore the stochastic nature of electrospinning could be balanced with the high number of total rotations. If the circumferential velocity of the drum is high, fibers can be oriented to the direction of the velocity and if the velocity is decreased, no significant change can be observed in the structure [25], therefore the circumferential velocity was set to a low value (0.2 m/s). The diameter of the rotating drum was 80 mm. The distance between the collector's surface and the spinneret was 120 mm. A power supply with a voltage adjusted at +25 kV DC was used for the experiments.

The PA-6 solution was supplied by a syringe pump (Aitecs SEP-10S plus, Lithuania) with a flow rate of 0.3 ml/h. Electrospinning was carried out at 35 °C, the relative humidity was between 40 and 50%.

Mat stripe-shaped samples were carefully cut in the direction of the rotation by sharp blade. The width of the samples was 6 mm and their length was at least 20 mm in every cases. Paper frames with a gap distance of 10 mm were cut from paper. The sample stripes were stuck to the frame by adhesive tape. The cross section of each sample was

estimated by measuring the area and weight of the sample and by the known density of the bulk material.

The tensile tests were carried out by Zwick Z005 (Germany) universal tensile tester, equipped with a force sensor which had a maximum load of 20 N and a resolution of 0.001 N. The test speed was 2 mm/min and the gauge length was 10 mm according to the paper frame size. In the course of the tensile tests the paper frame was inserted into the gripping equipment and then the edges of the frame were removed with the aid of scissors, therefore only the nanofibrous specimen remained between the grips. The total number of 80 samples were tested and the related displacement and force values were recorded, respectively.

The whole tensile process was analyzed by using FiberSpace software [21-23]. For the modeling, it was necessary to normalize the stress and the strain values. It means that the fiber stresses should be divided by the average fiber breaking stress and the strains must be divided by the average strain level at fiber break. It means that in this normalized plane of stress and strain the average fiber breaks at (1,1) coordinates and the modulus of every FBC is 1. The average value of single nanofiber breaking stress can only be determined from real single nanofiber measurements, therefore the normalization was only an approximation based on the least square method and on the basis of former experiments on microfibers [20]. The inaccuracy in the normalization was taken into account during the modeling as the whole curve could be shrinked or enlarged. The software automatically made this correction when finding the best-fitting curve and gave this zoom-ratio back as a constant. After the modeling, the results could be transformed back to real stress and strain values by multiplying by the above-

6

mentioned zoom-ratio and then by the normalization constants. The software tried to find the best fitting curve for the average tensile process diagram, automatically.

Scanning electron microscopy (SEM) was carried out by JEOL 6380 LA (Japan) instrument. To investigate the structural changes at different strain rates a simple sample preparation method was used. The tensile tests were stopped at appropriate displacement values. Then the specimen was watchfully attached to electrically conductive tape and carefully removed from between the grips, therefore the structure could be frozen at that current strain rate. Finally the specimen was sputtered with Au/Pd alloy and put into the vacuum chamber of SEM. Samples were analyzed at different strain rates, such as: 0,10…40%. The SEM micrographs were compared to the modeling results.

### 3. Results and Discussion

Nanofibers were successfully electrospun from the PA-6 solution. Scanning electron micrographs (SEM) of the samples can be seen in Fig. 2. Defect-free fibers, without any beads or droplets could be obtained. The average diameter of nanofibers was approximately 200 nm with low deviation.

The tensile stress and strain curves were calculated from the force – displacement functions. Fig. 3. shows five randomly selected tensile curves out of the 80 measurements. It can be seen that the tensile curve of nanofibrous materials have general characteristics. In the first stretch the curves are linear and have a high slope. In the next section the stress still increases in a linear, but degressive way. The transition between the two sections is not pointed. The breakage happens in the last section where the tensile stress suddenly drops off. The tensile modulus has a deviation and so does

the rise of the curve in the second stretch. The beginning and the end of the breakage can also be characterized by statistical ways.

The average tensile process was determined by calculating the average stress as a function of the strain. For this calculation all the measurements were added together point by point then divided by the number of specimens. The result had been a curve which was smoothened with the method of moving averages. The average tensile behavior is demonstrated in Fig. 4. The deviations of the stress values were also computed point by point, and depicted in the same chart. The real tensile processes mostly take place within this confidence interval as it is demonstrated by a real measured tensile curve (see Fig. 4.). The curve of the average process and the real measurement has same shape until the last section of the damage process. In case of the real samples the stress values drop off strictly but in case of the average curve the damage seems to be less jump-like. It is because the strains at break have a high deviation which appears as a slope in the calculated average curve. However, modeling the whole process could be carried out for the average curve, because it represents more information than only one sample about the structure. This kind of difference must be considered and taken into account when the damage process of the structure is analyzed in detail.

The result of modeling the average tensile process is depicted in Fig. 5. The two curves were delayed to each other for the sake of better visibility. The square of difference between the modeled and the calculated average tensile curve was calculated point by point and added together. It was found that the root of this sum (the error of modeling) was less than 0.003, thus the modeling curve fits well. From the modeling software all statistical parameters representing the FBCs could be retrieved and the fraction of each

bundle type could also be concluded. The most important FBC within the structure was found to be ES which takes 72 percent of the structure, while ET bundles gained 21.5 percent. The remaining 6.5 percent was E cell and no EH fibers were found. It means that the most important behavior during the tensile process is that bondings between the fibers break up and then fibers slip on one another, which is realized through frictional forces. Oblique fibers also take an important role in the tensile process as they are elongated and arranged according to the pulling axis then finally break. The fraction of each FBC is depicted in Fig. 6. This diagram is weighted by the fraction of the FBCs (note: FBCs have the same modulus, the difference in their slope is only caused by their different fraction).

The software also gave the modeling parameters for each fiber bundle cell. All parameters were got in the normalized plane of strains and stresses and are relative to the average fiber breaking strain therefore these values must be denormalized to get real values.

The slipping fibers (ES FBC) are the most dominant in the structure. This FBC have parameters, such as: ES, VS, EL, VL. The first one, ES is the average strain level where fibers begin to slip on each other and VS is its normalized deviation. EL is the average free slipping length which expresses the difference in strain levels where fibers begin to slip and where slipping stops due to the fiber endings or other material discontinuity. VL is the normalized deviation of EL parameter.

ES and VS was 0.23 and 0.18, EL and VL was found to be 0.96 and 0.12, respectively. If we denormalize these values we find that fibers within ES FBCs begin to slip at 8.3 ± 6.5% relative strain and the slipping stops at 34.7 ± 4.3% due to material discontinuity problems.

The oblique fibers (ET FBC) which is also important in the breaking process can be described by VE, ET, ST parameters. ET is the average obliquity of fibers and clearly depends on the geometry of the fiber structure and the tangent of the average angle between the axis of the fiber and the pulling direction. The obliquity has a deviation, ST. The model allows taking the fibers contraction into account, but in our case these parameters were found to be zero and therefore not explained in detail. ET was 0.53 and ST was 0.07 which means $28 \pm 4$ degrees relative to the pulling axis. VE which is the relative deviation of the average fiber strain at break was found to be 0.04 (which counts 1.45% when denormalized).

The E FBC can be described by VE parameter only, which is the same for every FBC. The average single nanofiber's strain at break was set to 1 during the normalization. If these values are transformed back, it means that the fiber breaking strain was $36.1 \pm 1.45\%$ in case of the E FBC.

When every parameter is known the whole damage process is revealed and can be described as follows. In the beginning of the tensile process the mat structure behaves according to Hooke's law, and without considerable structural changes. If the stress is increased above a critical level, two different phenomenons can happen where fibers cross each other: the weaker fiber breaks or the bonding between the fibers break up and nanofibers begin to slip on each other. In case of our material the latter one is the typical, the tensile curve characteristics shows that slippage occurs. The average fiber breaking force is significantly higher than the force needed for slippage, thus bonding between fibers begin to break up at an average strain value of 8.3% where the tensile stress reaches 17 MPa. In-axis (E) and oblique (ET) nanofibers can still bear tensile load which leads to a still linear, but less gradient slope. If the deviation of the bonding

10

breakup-stress would be zero, the transition between the two linear stretches of the tensile curve would be point-like break. The deviation of fiber diameters is small but that of the crossing angle of fibers in contact is rather large and quality of the bonding between the fibers can also be different, therefore in our case a long transition was observed. The deviation of the strain where bondings broke was 6.5%. The ES cell breaks at $34.7 \pm 4.3\%$ strain which leads to a slight, but continuous decrease in the stress. The damage of E and then ET cells appears in the average tensile curve as a smaller and then bigger decreases in the stress. The overall damage process takes place gradually in average. For modeling a composite bundle created by parallel connected FBCs was used and on the basis of results it was found that the E, ES and ET FBCs played a significant role therefore the EH FBC could be neglected. In the FBC model all the fibers or fiber chains were gripped at their both ends. If the structure is uniform along the length then the breakage happens according to this result of modeling. If there are small inhomogeneities such as deviance in the cross section or even in the microstructure which is an accompany of real nonwoven structures, it can lead to sudden breakage. It is because if we connect several FBCs or composite bundle of FBCs in serial then it constitutes a chain of fiber cell structures. If one segment of this fiber chain is weaker it can lead to breakage irrespectively of all the other, less-damaged cells. That is why the real specimens broke suddenly.

Fig. 7. shows a tensile curve and indicates five specific points (A-E) where the SEM micrographs were taken. Note, that the analysis was carried out on five different samples, thus the curve just demonstrates which typical stages of the tensile processes were analyzed. The first one is A, taken at zero elongation. B is taken where it is believed that bondings between fibers are breaking on the basis of modeling results, C

and D are taken in the second linear part of the tensile curve and E where fibers begin to break.

Fig. 8. shows one SEM micrograph for each specific point. At zero elongation no orientation can be observed and in case of the selected transition-point (B) the structure still does not undergo apparent structural changes. It confirms the assumption that slipping begins in this section, in so far as no fibers broke, no fiber endings can be seen. In the third point (C) the structural changes still do not seem to be considerable, but at 30% strain (D) some orientation of the fibers can be seen in the direction of the pulling axis. The damage of the real structure happens very suddenly, therefore sample with broken fibers (E) could not be prepared in order to characterize this phase by SEM. It means if only some fibers break it would decrease the cross section which leads to immediate break of the specimen. The stretched fibers here act as independent structural elements without significant frictional moving between them.

According to the modeling results the fiber strength utilization was found to be 0.386. It means that that the tensile strength of the mat is 38.6% of the tensile strength of single, well-gripped (E-type) nanofiber. The tensile strength of single nanofibers are resulted $85.5 \pm 3.4$ MPa. The tensile strength of nanofibrous mats, single nanofibers and the bulk material (4 x 10 mm dumbbell specimens) are compared in Table 1.

| | Nanofibrous mat | Single nanofiber | Dumbbell specimen |
|---|---|---|---|
| Tensile strength | $34.9 \pm 5.6$ MPa | $85.5 \pm 3.4$ MPa | $57.8 \pm 0.3$ MPa |

Table 1. The mechanical properties of different forms of PA-6

The theoretical tensile strength of single nanofibers is 48 percent higher than the bulk materials. This result fits well with the paradox of fibers which says that decreasing the fiber diameters would lead to increase in strength.

### 4. Conclusions

PA-6 nanofibrous mats were successfully electrospun with the aid of rotating drum collector. Determining the mechanical properties and behavior of a single fiber which has a diameter of only a few hundred nanometers is very complicated and therefore needs special and mostly expensive testing apparatus. In this paper instead of testing single nanofibers, nanofibrous mat samples were tested. Tensile tests were carried on 80 specimens and the results were modeled by FiberSpace software which is based on the theory of fiber bundle cells (FBCs).

The results of the modeling show that the structure is built up of nanofibers which can be straight or oblique relative to the axis of pulling. The most important phenomenon during the damage process is that bondings between the fibers can break up and then these fibers can slip on one another which manifests as frictional forces. At higher strain rates oblique fibers are highly oriented. The modeling results also fit well with the SEM analysis of the structure which gave a hand to reveal the structural changes during the whole damage process.

The stress limits which cause the fibers slipping and breaking were determined with the aid of the modeling software as well as the relative fraction of the different FBCs within the mat structure. Slipping fibers (ES FBC) took 72 percent of the structure, while oblique (ET FBC) bundles gained 21.5 per cent. The remaining 6.5 per cent were straight fibers (E FBC).

The tensile properties of single fibers could be estimated in view of the tensile properties of the fiber mat. The fiber strength utilization was 0.386 and the tensile strength of single nanofibers was found to be $85.5 \pm 3.4$ MPa based on the modeling results. Moreover it is 48% higher than the bulk PA-6 material has which fits well with

13

the paradox of fiber diameters. The quality of the structure and the tensile behavior could be concluded from tensile tests and modeling only and not from other, more complicated tests or without using any expensive apparatus.

**Acknowledgement**

**References**

1. Moniruzzaman M, Winey KI. Polymer nanocomposites containing carbon nanotubes. Macromolecules 2006; 39(16):5194–5205.

2. Romhany G, Szebenyi G. Interlaminar crack propagation in MWCNT/fiber reinforced hybrid composites. Express Polym Lett 2009; 3(3): 145-151.

3. Cao G, Chen X, Xu ZH, Li X. Measuring mechanical properties of micro- and nano-fibers embedded in an elastic substrate: Theoretical framework and experiment. Compos Part B-Eng 2010; 41(1): 33-41.

4. Xin Y, Huang Z, Chen J, Wang C, Tong Y, Liu S. Fabrication of well-aligned PPV/PVP nanofibers by electrospinning. Mater Lett 2007; 62(6-7):991-993.

5. Teo WE, Gopal R, Ramaseshan R, Fujihara K, Ramakrishna S. A dynamic liquid support system for continuous electrospun yarn fabrication. Polymer 2007; 48(12):3400-3405.

6. Smit E, Bűttner U, Sanderson RD. Continuous yarns from electrospun fibers. Polymer 2005; 46(8):2419–2423.

7. Bazbouz MB, Stylios GK: Novel mechanism for spinning continuous twisted composite nanofiber yarns. Eur Polym J 2008; 44(1):1-12.

8. Andrady AL. Science and technology of polymer nanofibers. Hoboken: John Wiley & Sons Inc., 2008.

9. Chang ZJ, Zhao X, Zhang QH, Chen DJ. Nanofibre-assisted alignment of carbon nanotubes in macroscopic polymer matrix via a scaffold-based method. Express Polym Lett 2010; 4(1):47-53.

10. Heikkilä P, Harlin A. Electrospinning of polyacrylonitrile (PAN) solution: Effect of conductive additive and filler on the process. Express Polym Lett 2009; 3(7):437-445.

11. Taepaiboon P, Rungsardthong U, Supaphol P. Vitamin-loaded electrospun cellulose acetate nanofiber mats as transdermal and dermal therapeutic agents of vitamin A acid and vitamin E. Eur J Pharm Biopharm 2007; 67(2):387-397.

12. Nagy ZsK, Nyúl K, Wagner I, Molnár K, Marosi Gy. Electrospun water soluble polymer mat for ultrafast release of Donepezil HCl. Express Polym Lett 2010; 4(12):763-772.

13. Huang FL, Wang QQ, Wei1 QF, Gao WD, Shou HY, Jiang SD. Dynamic wettability and contact angles of poly(vinylidene fluoride) nanofiber membranes grafted with acrylic acid. Express Polym Lett 2010; 4(9):551-558.

14. Yang DZ, Zhang J, Zhang JF, Nie J. Preparation and characteristics of oriented superparamagnetic polymer nanofibres. Plast Rubber Compos 2010; 39(1):6-9.

15. Reneker DH, Yarin AL. Electrospinning jets and polymer nanofibers. Polymer 2008; 49(10):2387-2425.

16. Ding Y, Zhang Y, Jiang Y, Xu F, Yin J, Zuo Y. Mechanical properties of nylon-6/$SiO_2$ nanofibers prepared by electrospinning. Mater Lett 2009; 63(1):34-36.

17. Yang L, Fitié CFC, Werf KO, Bennink ML, Dijkstra PJ, Feijen J. Mechanical properties of single electrospun collagen type I fibers. Biomaterials 2008; 29(8):955-962.

18. Lee SH, Tekmen C, Sigmund WM. Three-point bending of electrospun $TiO_2$ nanofibers. Mater Sci Eng A Struct Mater 2005; 398(1-2):77-81.

19. Vas LM, Rácz Zs. Modelling and testing the fracture process of impregnated carbon-fiber roving specimens during bending: Part I – Fibre bundle model. J Compos Mater 2004; 38(20):1757-1785.

20. Molnár K, Gombos Z, Vas LM. Testing and Modeling the Tensile Strength Behavior of Glass Fibers, Fiber Bundles and Fiber Mat. Mater Sci Forum 2008; (589):227-232.

21. Vas LM, Tamás P. Modelling Method Based on Idealised Fibre Bundles. Plast Rubber Compos 2008; 37(5/6):233-239.

22. Vas LM, Tamás P. Modelling Failure and Size Effect of Oriented Polymers by Fiber Boundle Based FiberSpace. In: Proceedings of the 9th World Textile Conference AUTEX. Izmir, May, 2009. p.1289-1297.

23. Vas LM, Tamás P. Modelling Size Effects of Fibrous Materials Using Fibre-Bundle-Cells. In: Proceedings of the 14th European Conference on Composite Materials ECCM-14. Budapest, June, 2010. CD-issue, p11.

24. Molnár K, Provost M, Vas LM. Electrospinning and characterization of polyamide nanofibrous mats. In: Proceedings of the 3rd Aachen-Dresden International Textile Conference. Aachen, November, 2009. CD-issue, p7.

25. Li WJ, Maucka RL, Cooper JA, Yuana X, Tuan RS. Engineering controllable anisotropy in electrospun biodegradable nanofibrous scaffolds for musculoskeletal tissue engineering. J Biomech 2007; 40(8):1686–1693.
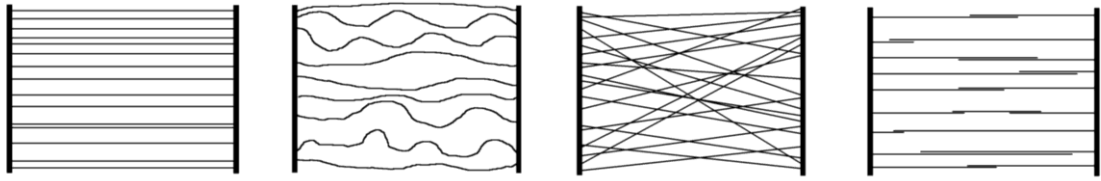
Fig. 1.: Idealized fiber bundle cells (from left): E, EH, ET, ES [20].
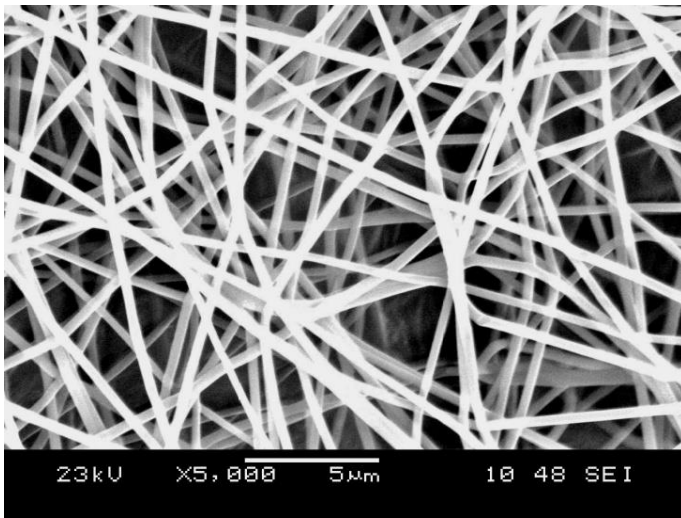


Fig. 2.: SEM micrograph of electrospun PA-6 nanofibrous mat
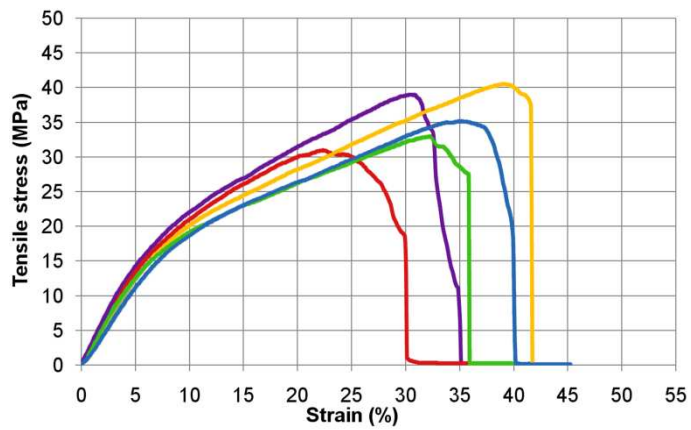


Fig. 3.: Tensile behavior of nanofibrous mat stripe samples
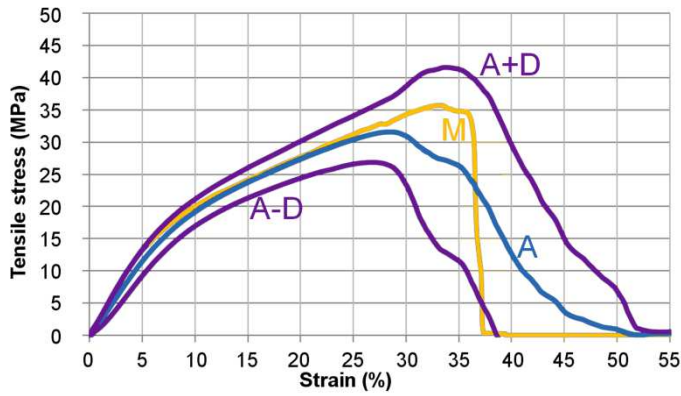
Fig. 4.: Average tensile behaviour of nanofibrous mats compared to a real measurement.

A: average tensile curve, A+D: average tensile curve plus deviation, A-D: average

tensile curve minus deviation, M: a real measurement
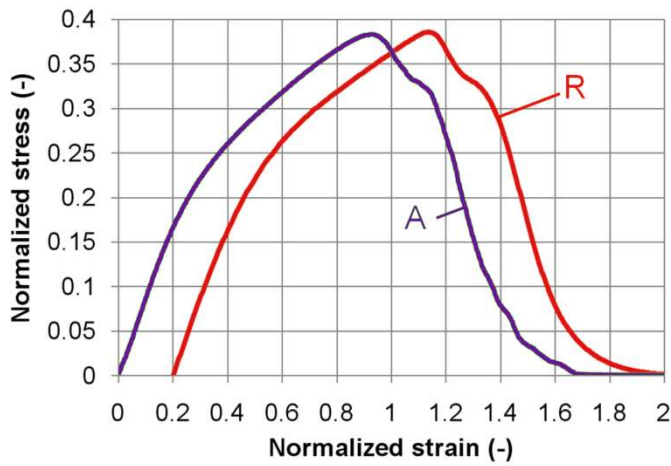


Fig.5.: Modeled average tensile curve. A: average tensile curve destined for modeling,

R: the result of the modeling



18
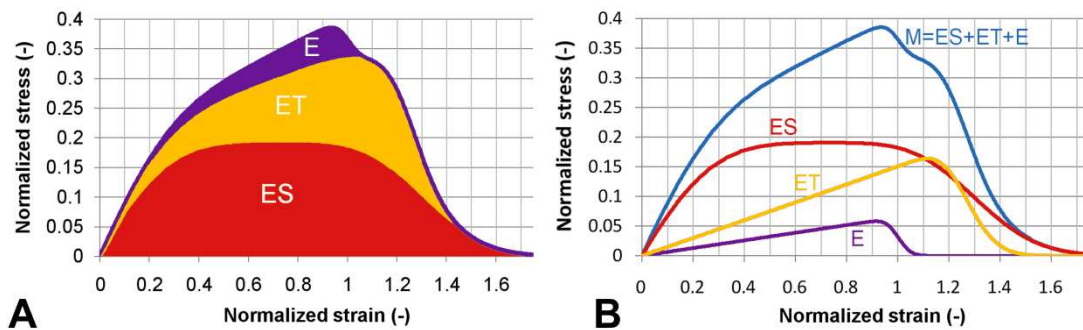
Fig. 6.: Decomposition of the modeled average tensile process. A: the sum of the tensile processes of ES, ET and E FBCs is the modeled average tensile process. B: the tensile curves of E, ET, ES and the modeled (M) curve are depicted separately.
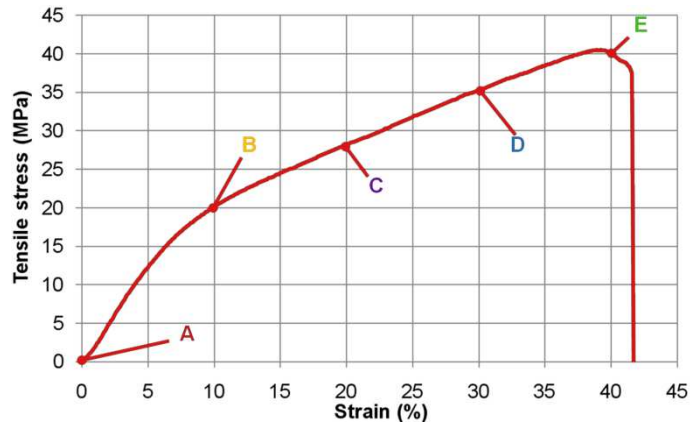


Fig. 7.: Tensile curve of a selected sample and the specified points (A-E) where the SEM analysis was carried out
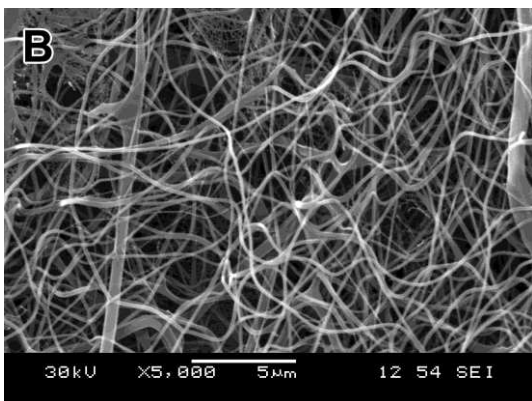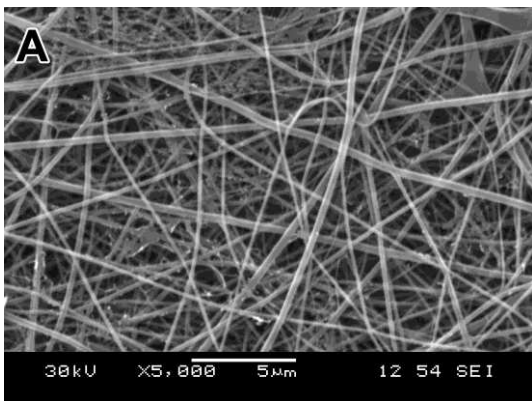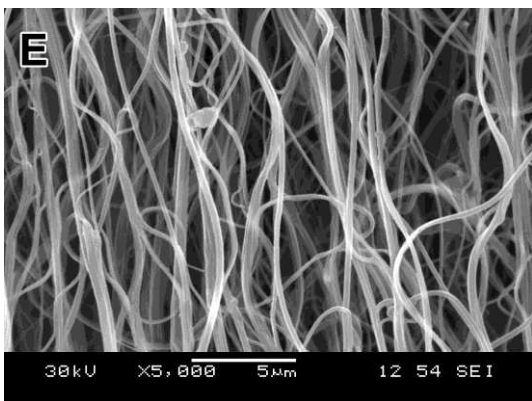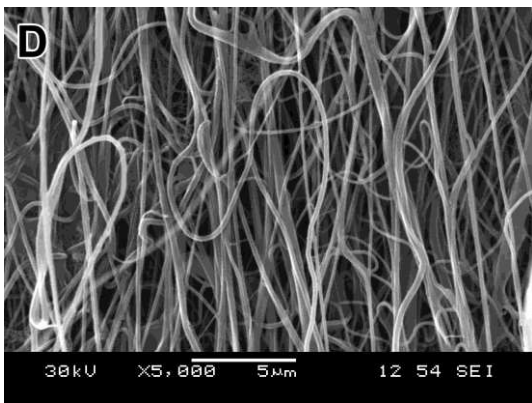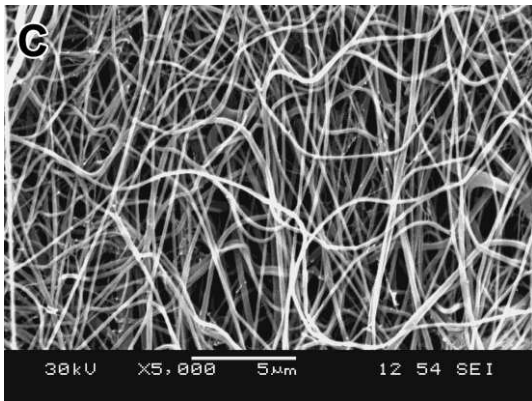
Fig. 8. Scanning electron micrographs of the electrospun PA-6 samples taken at different nominal strains - A: 0%, B: 10%, C: 20%, D:30%, E:40%